



Journal of Advanced Zoology

ISSN: 0253-7214

Volume 43 Issue S -01 Year 2022 Page 425:438

Detected Genetic Markers for Three Varieties of Rice (*Oryza sativa* L.) under Nano- Particles

Sozan Eid El-Abeid¹, Samy A. A. Heiba², Ibthal S. El-Demerdash², Maha S. A. Haridy³, Shadia Sabry⁴, Shimaa E. Rashad^{5*}

¹Mycology and Disease Survey Research Department, Plant pathology Research institute, ARC, Egypt

²Genetics and Cytology Department, Biotechnology Research Institute, National Research Centre.

³Central Lab of Organic Agriculture, Agricultural Research Center

⁴Botany and Microbiology Department, Faculty of Science, AL- Azhar University, Cairo, Egypt

^{5*}Microbial Genetics Department, Biotechnology Research Institute, National Research centre, Giza, Egypt.

***Corresponding Author:** Shimaa E. Rashad

^{*}Microbial Genetics Department, Biotechnology Research Institute, National Research centre, Giza, Egypt.

Article History	Abstract
<p>Received: 26 July 2023 Revised: 12 Sept 2023 Accepted: 26 Oct 2023</p>	<p><i>Despite the enormous advancements in breeding, fresh and accessible methods of plant development are preferred. Many research have been done to determine the impact of zinc oxide nanoparticles (ZnO NPs) and magnesium nanoparticles (MgONPs) on plant growth. ZnO NPs and MgONPs have been used extensively in agriculture. Few research have looked into the potential impact of ZnO NPs on grain Zn content or cereal yield formation to date. The goal of the study was to demonstrate how varied concentrations of nanoparticles affected root germination in three different rice types (Giza 177, Sakha super 300, and Sakha 108) and the fungus Fusarium moniliforme, which causes foot rot in rice. Here, we performed a pot experiment to assess the effects that ZnO nanoparticles and MgONPs had on the shoot length, root length, and germination of rice. The experiment involved three dosages of Zn and Mg nanoparticle solution at varying concentrations of 10, 20, and 100 ppm. The outcomes showed that, when compared to the control treatment, ZnO NPs and MgONPs increased the length of the shoot, the length of the roots, and the rate of germination. Using random amplified polymorphic DNA (RAPD) and inter simple sequence repeats (ISSR) markers, the genetic makeup of plants treated with 10, 20, and 100 ppm AgNPs was also examined. In vitro rooted shoots were acclimated in a greenhouse before being tested for biochemical stability and phenotypic stability. In vitro, callogenesis and caulogenesis were both reduced by AgNPs at the greatest dose (100 ppm). In order to maximise genome coverage, three rice cultivars from distinct origins were chosen, and they were tested using three RAPD markers and seven selected ISSR markers. AgNPs- treated plants using ISSR markers produced 87 amplified bands in total, 45 polymorphic allelic variants, and 36 monomorphic allelic variations. The Pearson correlation coefficient was used in the Mantel test to determine whether there was a significant</i></p>

<p>CC License CC-BY-NC-SA 4.0</p>	<p>association between the Jaccard's dissimilarity matrices based on ISSR and RAPD markers ($r = 0.69$; $P 0.05$). Morphological characteristics, ISSR, and RAPD analysis were used to partition the UPGMA Dendrogram into two groupings. Jaccard's coefficient was used to analyse the genetic similarity matrix. Sakha Super 300 and Giza 177 had the most genetic similarity (95%) while Sakha 108 and Giza 177 had the lowest genetic similarity (90%) according to ISSR and RAPD study. The classification of rice germplasm, breeding initiatives, and conservation efforts all heavily rely on the determination of genetic diversity within the rice species. To find genetic variations, morphological characteristics, ISSR, and RAPD analysis are useful techniques. The findings demonstrated the large ratio of variation in rice. This work successfully established the possibility of using MgONPs and ZnO NPs as high-performing fertilisers to improve rice output and quality. This study could serve as a guide for future research on rice and could support efforts to understand the species and improve breeding stock.</p> <p>Keywords: ZnO NPs, MgO NPs, Nanotechnology, ISSR-PCR, RAPD-PCR, <i>Fusarium moniliforme</i>,</p>
--	--

1. Introduction

For the majority of the world, rice (*Oryza sativa* L.) is an essential cereal food crop (Khush, 2005; Khan et al., 2022). Being heavy in carbs, low in fat, and abundant in calories, protein, and vitamins gives it great nutritional advantages (El-Mowafi et al., 2021). Its area is almost 162 million hectares, and it will produce 756 million tonnes by the year 2022 (Faostat). Additionally, in order to deal with the threat of environmental challenges and the ongoing population growth, this production should be enhanced (Fageria, 2007).

The development of nanotechnology has provided favourable applications for sustainable agriculture. The agriculture sector faces numerous and unprecedented challenges, such as decreased crop yields due to biotic and abiotic pressures, including nutrient deficiencies and pathogenic bacteria. It is a relatively new practise to utilise nanoparticles to enhance plant development and reduce plant diseases (Rastogi et al., 2019). However, the problem of phytotoxicity brought on by NP exposure remains unclear. Recent studies (Youssef and Elamawi 2018) revealed a considerable effort to understand how nanoparticles affect plant growth and suggested a favourable impact of NPs on plant development with the potential to be employed as nano-fertilizer in the future. More than half of the world's population depends heavily on rice (*Oryza sativa* L.), therefore to keep up with expanding demand, rice production needs to double by 2050 (FAO 2009).

Rice is a staple food for many people because of its high content of proteins, minerals, vitamins, and fibres. However, rice is susceptible to various fungal diseases, such as rice foot rot disease caused by *Fusarium verticillioides* (formerly known as *F. moniliforme* or *Gibberella fujikuroi*) (Nirenberg, 1976 Ou, 1985, Couch and Kohn 2002). This seed-borne fungus can cause 10–30% of the world's rice crop loss (Nalley et al., 2016). The majority of rice cultivars are vulnerable to several fungal races. Fungicides are frequently used to control blast, but they are losing favour because they raise the risk of *M. oryzae* developing fungicide resistance and because they run afoul of public concerns about the effects of fungicide residues on human health and the environment.

Controlling the disease is difficult because the fungus is so varied (Ou 1985). Using nanoparticles as an alternative could help regulate this illness. According to Young et al. (2009), Elamawi and El Shafey (2013), and Elamawi et al. (2018), silver nanoparticles are used successfully to reduce rice blast and avoid harmful infections in rice. ZnO NPs have been shown to have antifungal activity against a variety of fungus species by a number of researchers, including He et al. (2011), Gunalan et al. (2012), Wani and Shah (2012), Savi et al. (2013), Elamawi et al. (2016), and Sierra Fernandez et al. (2017). As far as we are aware, there have been no reports of ZnO NPs being used to control *M. oryzae*.

When used as a fertiliser, ZnO NPs may be more readily available to plants than standard Zn fertiliser, which could result in improved rice growth. According to Kulhare et al. (2017), foliar Zn fertiliser application increased rice productivity and grain Zn concentration. Due to its special qualities, such as biodegradability, non-toxicity, suppression of biofilm growth, degradation of hazardous colours such as methyl violet, and many more (Fernandes, et al., 2020), magnesium oxide nanoparticles have become a promising contender for

solving a variety of problems.

In the current work, ISSR markers have been employed to ascertain the genetic diversity among various Hassawi rice landraces. In order to produce polymorphic DNA bands in the rice genome, the effectiveness of ISSR primers of di- and tri-nucleotide repeats has been investigated (Al-Turki et al., 2015).

The outcomes demonstrated that RAPD primers generated 49 bands with a size range of 0.1-3 kb and an 87.75% polymorphism proportion. For RAPD, 43 polymorphic bands with distinguishable bands were discovered. According to morphological traits and RAPD analysis, the UPGMA Dendrogram was classified into three groups (Rashad et al., 2023).

Determining how various medium compositions affect the regrowth and embryogenic responses of various barley genotypes. The three barley genotypes El-kasr, G126, and G130 were successfully evaluated for the presence of somaclonal variation using biochemical and molecular genetics examinations of protein, isozymes, and RAPD-PCR (Rashad et al., 2020; Rashad et al., 2023). the capacity of RAPD markers to identify relationships between diverse genotypes and demonstrate how yield metrics at the molecular level are related. In order for barley breeders working with gene banks to ensure that it can be produced sustainably and utilised to its fullest extent, it is imperative to understand the diversity of barley. Using cutting-edge molecular, biochemical, and physiological techniques, this can be accomplished by thoroughly phenotyping and genotyping the barley collections (Merwad et al., 2020). ISSR analysis and physical features can be used to find genetic variations (Shata *et al.*, 2021). SSR marker analysis is less effective than ISSR markers at detecting genetic diversity among the evaluated cultivars of Alfalfa. In comparison to the SSR marker, the ISSR marker is more precise and yields more data (Heiba et al., 2022). ISSR primers produced 37 bands with widths ranging from 100 to 2000 bp and an 87.5% success rate, proportion of polymorphism. Polymorphic information content (PIC) for ISSR was 0.74. The UPGMA Dendrogram was divided into two clusters based on physical characteristics, and ISSR analysis is a helpful tool for locating genetic variations, Rashad et al 2022.

Using molecular markers ISSR and RAPD, the current study aims to assess the effects of ZnO and MgO nanoparticles on the germination of three different rice varieties (Giza 177, Sakha super 300, and Sakha 108) and the fungal activity *Fusarium moniliforme* in rice that causes foot rot. Additionally, to research the potential impacts of varying ZnO NP application rates as a nano-fertilizer and anti-fungal agent to reduce rice *Fusarium moniliforme* and increase cultivar grain productions.

2. Materials And Methods

Synthesis of Zinc and Magnesium Nanoparticles from different precursor

90 ml of 10mM each of zinc sulphate, magnesium sulphate and magnesium chloride separately were added drop by drop to 10 ml of 25% *Eucalyptus melliodora* (camphor (ca)) aqueous extract in a 250 ml Erlenmeyer flask. For 30 minutes, the mixture was heated on a magnetic stirrer at 80 °C while being continuously stirred. After a while, NPs started to form and the colour changed from white to greyish white. For 30 minutes, 6000rpm of centrifugation was used to separate the nanoparticles. After discarding the supernatant, the pellet underwent three centrifugal washes in distilled water. After being dried for 24 hours at 60 °C in a vacuum oven, the residue powder was characterised using a variety of methods.

Characterization of Zn and Mg-nanoparticles. XRD and UV-Vis Spectra Analysis

Spectra were analysed using a double-beam spectrophotometer (model 8453E, HP). After dilution into deionized water, a tiny aliquot of the NPs solution was used to measure the UV-Vis spectrum of the reaction solution in the 200-600 nm wavelength range. At room temperature, the solution was examined after being pipetted into a test tube.

Transmission Electron Microscope (TEM) and DLS

A transmission electron microscope (JEOL 100CX II, Japan, with an accelerating voltage of 100 kV) was used to examine several NPs. Drops of an aqueous solution of NPs were placed on carbon-coated copper grids to create nanoparticles for TEM investigation, which were then allowed to dry for five minutes before the excess solution was blotted away with blotting paper at room temperature. And confirmed with dynamic light scattering (DLS).

Fourier Transform Infrared Spectroscopy (FT-IR)

FT-IR spectra were analysed using a data station-equipped BOMEM FT-IR Spectrometer (MB 147, Canada) in the range of 4000 to 400 cm⁻¹. About 100 mg of dried samples and 100 mg of spectral grade KBr were combined, and then the mixture was pressed into discs using hydraulic pressure.

Isolation and purifications of seed borne fungi:

Rice seeds were sterilised for two minutes by being submerged in a solution containing 0.5% sodium hypochlorite (NaOH) in order to cultivate and isolate the fungus. A sample is placed on a medium made of potato dextrose agar (PDA) after being washed twice with sterile distilled water. The plates underwent a 5- to 7-day incubation period at a temperature of 25°C. The growing fungus were then refined via the single-spore method.

Identification:

Using the key of imperfect fungi (Barnett and Hunter, 1972); and of *Fusarium* sp. (Nelson et al., 1983), the isolates of the fungus were identified based on their morphological traits and microscopic examination. The fungal isolate was placed into glass flasks containing 100 mL of potato dextrose broth prior to DNA extraction. The flasks were then continuously shaken until mycelium had developed. To get rid of any traces of the culture medium, the mycelia were collected, filtered through cheesecloth, and then repeatedly washed with sterile distilled water.

Using a Disposable Pellet Pestles, 50 mg of fresh mycelia from the fungal isolates were mechanically broken apart in order to extract the DNA and do PCR sequencing. The Jena Bioscience DNA extraction kit was then used to extract the entire sample's DNA. Following a dilution procedure to isolate the DNA from its surrounds, the nuclear ribosomal DNA's ITS sections were amplified using the primers ITS1F- 4, as explained by Gardes and Bruns in 1993. The ultimate volume of the polymerase chain reaction (PCR) was 20 L. The reaction mixture included 10 L of the amaR One PCRTM Gene DireX, Inc., 1 M of each primer, and 50 ng of template DNA. Mix master. The thermal cycling settings included an initial denaturation phase lasting two minutes at 94 °C, followed by 35 cycles of denaturation lasting one minute at 94 °C, annealing for 30 seconds at 58 °C, and extension lasting one minute at 72 °C. A final extension step was carried out for seven minutes at 72 °C. The results of the PCR were examined under UV light after electrophoresis on a 2% agarose gel coloured with Gel-Red (Biotium TM). With the aid of a solution containing 1 volume of 20% polyethylene glycol 8000 and 2.5 M NaCl, the PCR products were purified by precipitation. The primers ITS1F(5'- CTT GGT CAT TTA GAG GAA GTAA-3') and ITS4(5'-TCC TCC GCT TGA TAT GC-3') were used to perform forward and reverse sequencing on the PCR products that had undergone purification, in accordance with **White et al. (1990)**.

In vitro fungal activity and seed germination test

- Three different rice types, Giza 177, Sakha super300, and Sakha 108, were employed in the experiment. In each of the three huge petri dishes, 75 seeds of each variety were planted, with 25 seeds for each Nano-treatment/ replicate. The first treatment used a ZnO-NPs solution, which is represented by the letter (A). The second treatment used a high concentration Nano-magnesium solution, which is represented by the letter (B). The third treatment used a low concentration of MgO-NPs solution, which is represented by the letter (D). and repeated in pot experiment.
- Distilled water was used as the first irrigation for all experimental varieties. The treatments under study were then irrigated for a period of fifteen days using a regulator watering system, and the following measurements were made: the length of the shoot, the length of the roots, and the percentage of germination.

To investigate the impact of nanoparticles at various concentrations on rice plant seed germination. seeds that were exposed to solutions containing Zn and Mg nanoparticles at concentrations of 10, 20, and 100 ppm. To examine the effectiveness of synthesized nanoparticles as an antifungal agent, PDA plates were also treated with varied doses of 10, 20, and 100 ppm of Zn and Mg nanoparticle solution before being inoculated with *Fusarium moniliforme*.

DNA extraction of ISSR and RAPD reaction conditions:**DNA extraction: using DNA kit methods**

PCR results were shot using the Biometra - Bio Documentations gel documentation system and UV transilluminated using a 100 bp DNA ladder. According to the gel analyzer technique, the amplified bands were graded as (1) for all studied wheat types' presence and (0) for their absence. A list of 10 primers is shown in Table 1 for the purpose of finding polymorphism among the three rice cultivars. These primers were developed by ISSR-PCR in accordance with Williams et al.'s (1990) guidelines with a few minor modifications.

In PCR-ISSR tests, inter-simple sequence repeats (ISSRs) are utilized to identify ISSRs. The reaction mixture, which consists of 20 ml of standardization (20 ml of PCR buffer 1X, 2.5 mM MgCl₂, 1 mM dNTPs, 10 pmol primer, 1-unit Taq polymerase, and 50 ng genomic DNA; 38 cycles of 56 °C: 1 min annealing, 2 min extension, and 10 min final extension at 72 °C). The ISSR-PCR data will be analysed using a 1.4% (w/v) agarose gel. Heiba et al. (2022) will assess the size of the amplified bands using a 1Kb and 100bpDNA ladder from Ferments Life Sciences and a gel documentation device (Syngene™) to capture pictures of the gels.

ISSR-PCR analysis:

In PCR tests, ISSR primers will be utilized, according to Zietkiewicz et al. (1994). The extracted DNA will be used to run an ISSR-PCR reaction on numerous samples. The reaction mixture will consist of 2 l of genomic DNA, 1 l of the primer, 2.5 l of 10X Taq DNA polymerase reaction buffer, 1.5 units of Taq DNA polymerase, and 200 mM of each dNTP. The amplifications will be performed using a DNA amplification Thermo cycler (PTC-100 PCR version 9.0 from M J Research-USA). The equipment is set up to work in the following circumstances: a 5 min denaturation step at 94°C, followed by 35 cycles of 30 s at 94°C, 90 s at the annealing temperature (specified by each primer), and 90 s at 72°C.

For the amplifications, which will be performed at least twice in order to undertake further data analysis, only repeatable products will be used.

Electrophoresis on a gel using a DNA ladder (1Kb) in 1X TAE buffer, the ISSR amplification products will be separated on 1.5% agarose gels. The gels will next be identified by staining with ethidium bromide, in accordance with Sambrook et al., (1989). The PCR findings will be imaged and documented using the Biometra - Bio Doc. Analyze gel documentation system.

Electrophoresis and RAPD Analysis

Using five enhanced RAPD primers, the DNA of the sunflower germplasm was amplified using a polymerase chain reaction (PCR). To determine the genetic diversity among the sunflower varieties, RAPDs were utilized. Denaturation at 95°C for one minute, annealing at 36°C for one minute, and extension at 72°C for two minutes for 35 cycles comprised the three phases of the PCR. The PCR programmed was set up to keep the outcomes at 4°C. 6 l of loading dye (0.50% xylene cyanol and 0.50% bromophenol blue) were added to the goods and spun in a mini centrifuge. The PCR result was electrophoresed on a 2% agarose gel at a voltage of 100 V, and amplified bands were found on a gel documentation system by Bio-Rad (Hercules) (Rashad et al., 2020).

Data analysis: Only clear, unambiguous, and reproducible bands will be considered for data analysis. Every band will be handled individually as a locus.

Data will be rated as (1) for presence and (0) for absence for each of the seven samples of barley using the Gel analyser programme, which is used to identify positive and negative markers. In order to make a dendrogram using the unweight pair group approach with arithmetical average (UPGMA), the similarity coefficients will be generated by the SPSS programme version 10 (Norman et al., 1975).

Statistical Analysis

The data were statistically analysed in accordance with Gomez and Gomez (1984). The least significant differences (LSD) were used to compare treatment mean differences at the 5% and 1% levels of probability.

3. Results and Discussion

Characterization of Zn and Mg nanoparticles.

The green synthesis of ZnO-NPs by *Eucalyptus melliodora* (camphor (ca) was confirmed by dynamic light scattering; UV-Vis spectra analysis and X-ray diffraction (XRD). The UV-Vis spectra analysis, performed using a double-beam spectrophotometer (8453E, HP), showed an absorption peak of ZnO- NPs at 310 nm wavelength in the 200-600 nm wavelength range (Fig. 1). The size of ZnONPs was determined by dynamic light scattering and found to be 36.8 nm on average.

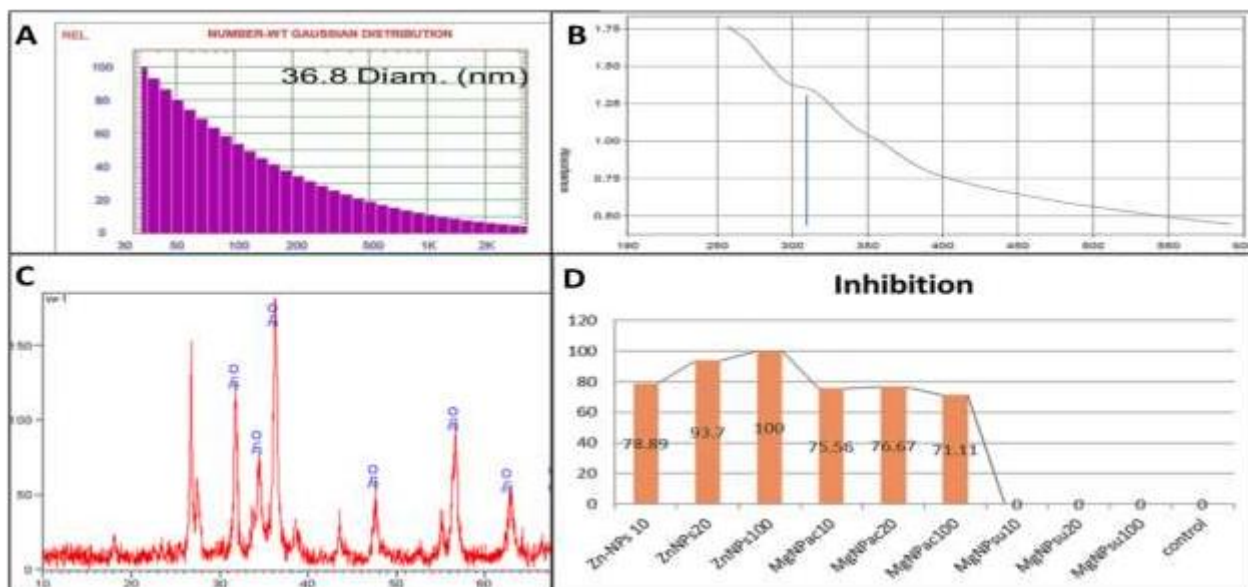


Fig. 1. Shows the Characterization of ZnO-NPs by Dynamic Light Scattering (A), UV-Vis Spectra analysis (B), XRD (C), and the histogram (D) indicate indicates the effect of ZnO-NPs on reducing the growth of *Fusarium moniliforme* that causes foot rot disease in rice, compared to other nanoparticle treatments.

TEM, or transition electron microscope.

The majority of the synthesised ZnO-NPs, which are shown in Figure (2A) to have an average size of 25 to 31.8 nm, appear to be spherical particles. However, the majority of the MgONPs (MgOac and MgOsu), which have 10-35nm for MgOac and 28-47nm for MgOsu, respectively, were synthesised from sulphate or acetate.

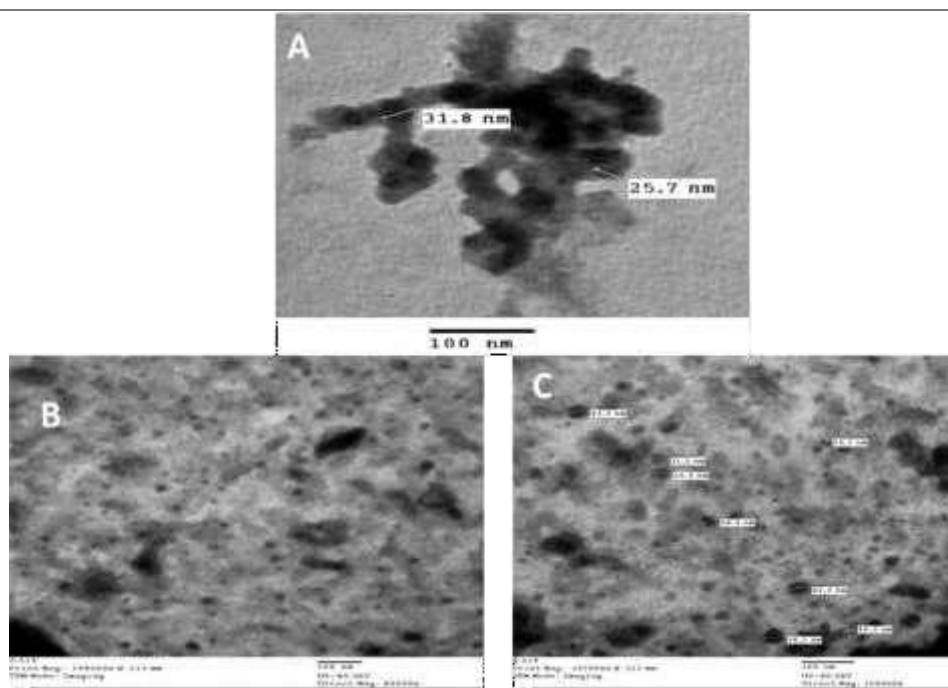


Fig. 2. TEM of ZnO-Zs-NPs(A) and MgO NPs (MgOac) Band MgONPs(MgOsu) C

Fourier Transform Infrared Spectroscopy (FT-IR)

Figure (3) showed that the FTIR results for nanoparticles made from sulphate or acetate precursor, such as ZnO-NPs or MgO-NPs. The FT-IR analysis was used to identify the substances and/or functional groups that are most likely present in the created nanoparticles. The ZnONP spectrum shown in Fig. 3A, which exhibits distinct peaks at 3188.67, 2345.33, 2153.2093, 1959.1613, 141.406, 605, and 453.67 cm^{-1} . The significant broad absorption peak at 3188.67 cm^{-1} is attributed to O-H stretching of carboxylic acid. While the peak at 1613 cm^{-1} is attributed to C=O stretching in amides or N-H bend from amides (primary amide), possibly

similar to amino acids or protein. The peak at 1063 cm^{-1} , and the peaks from 605 to 429, suggest the formation of ZnO. Potential secondary metabolites include tannins, saponins, terpenoids, and terpenes. The spectrum of MgO-NPs synthesized from acetate (MgOac) shown in Fig. 3B displays distinct peaks at 2103, 1437, 984, and 441 cm^{-1} . The spectrum of MgO-NPs synthesized from sulphate (MgOsu) shown in Fig. 3B also has a peak at 984 cm^{-1} . These peaks indicate the formation of MgO, in addition to the presence of other organic compounds.

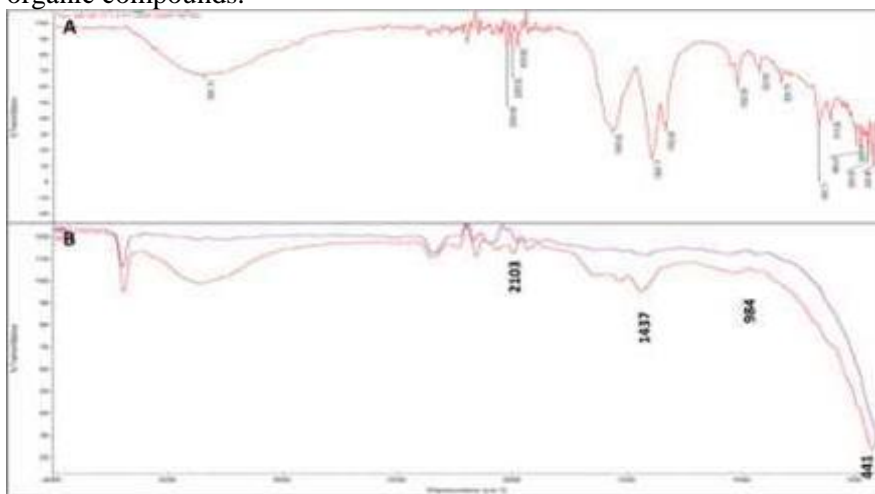


Fig. 3. FTIR of ZnO-NPs (A) and MgO-NPs synthesized from sulfate or acetate (MgOsu andMgOac) B

The isolation identification and cultivation of the fungus:

Fusarium moniliforme was identified and confirmed by DNA sequenced and submitted in NCBI by accession number OR523600.

In vitro seed germination

Figure (4) showed that the effect of zinc (Zn) and magnesium (Mg) nanoparticles (NPs) at different concentrations on rice seed germination. Seeds treated with of 10, 20, and 100 ppm of Zn or Mg NPs individually had a significant increase in length when compared to the control. however, when the concentration of Zn or Mg NPs increased, the shoot length decreased significantly. This indicates that Zn and Mg NPs have a positive effect on plant growth at certain concentrations, but a negative effect at higher concentrations.

In vitro fungal activity

When Zn and Mg nanoparticle concentration was increased, however, plant length significantly decreased, as shown in Fig. 4. This shows that while Zn and Mg nanoparticles have positive effects on the plant at certain concentrations, when that concentration is increased, this leads to toxic effects on plant growth, as shown in Fig. 3.

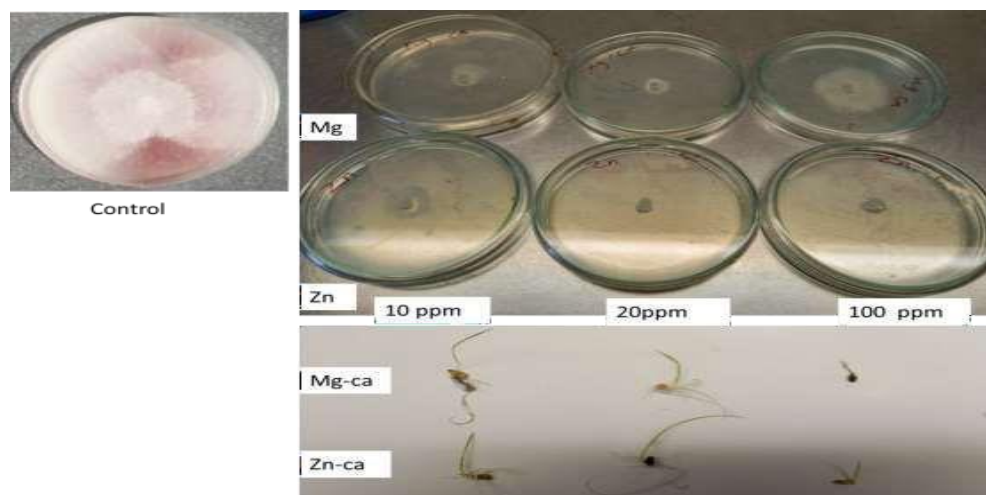


Fig. 4. Effects of Zn-NPs and Mg-NPs(ac) on *Fusarium moniliforme* growth and rice seed germination at different concentrations

Fungal growth has significantly decreased when Zn and Mg-NPs(ac) concentration was increased, as shown in Fig. 1. This indicates that Zn, and Mg nanoparticles have positive effects on the fungal growth when at all concentrations; however, when that concentration is increased, this has an unfavorable impact on the environment.

According to **Petosa et al. (2017)**, nanoparticles of various metal oxides can play a significant role in promoting plant development and yield as well as suppressing plant diseases. In the current study, it was found that, depending on the concentration and timing of applications, Zn NPs are more frequently linked to improvements in rice growth and yield when cultivated in pathogen-infected soil. All of the findings were unexpected considering that immature seedlings at the nursery were given a single dose to have a long-lasting, frequently season-long effect. These results are crucial for future field applications because they allow for the safe and regulated delivery of modest amounts of NPs to early seedlings, all while easing worries about NP exposure to both humans and the environment.

Effect of ZnO NPs on genomic DNA of Rice (*Oryza sativa* L.) using ISSR and RAPD-PCR primers:

In order to ascertain the impact of the various doses of ZnO-NPs and MgONPs utilised in this investigation, the genomic DNA of rice (*Oryza sativa* L.) was subjected to seven ISSR markers and three RAPD primers (Table 1 and Figures 5&6&7). Each and every one of the ISSR primers amplified and produced polymorphic alleles that displayed monomorphic alleles. In the meantime, three of the RAPD-PCR primers employed in this investigation amplified and produced polymorphic bands.

Table (1): ISSR and RAPD primers used for three rice amplification, the number of bands produced, unique bands and polymorphic band percentage

Molecular markers	Primers	Primers sequence (5'→3')	Monomorphic bands	Unique bands	Polymorphic bands	Total bands	Polymorphism%	Range of bands (bp)
ISSR	UBC809	AGA GAG AGA GAG AGAGG	4	1	1	6	20%	383:1084
	UBC823	TCT CTCTCTCTCTCT CC	4	2	4	8	50%	349:1403
	UBC807	AGAGAGAGAGAGAGAGT	6	2	4	10	40%	303:1377
	UBC889	DBDACACACACACACAC	4	2	3	7	42.86%	478:1363
	UBC834	AGAGAGAGAGAGAGAGYT	4	0	5	9	55.56%	318:1660
	UBC817	CACACACACACACAAA	4	1	3	7	42.86%	655:1519
	UBC873	GACAGACAGACAGAC	0	4	7	11	100%	518:1715
RAPD	SBSC18	TGAGTGGGTG	4	1	2	6	33.33%	490:1320
	SBSF14	TGCTGCAGG	5	2	5	10	50%	429:1511
	SBSE07	AGATGCAGCC	1	9	13	14	92.86%	510:1634

ISSR markers:

Five bands altogether, ranging in size from 383 to 1084 bp, were produced as a result of the samples' DNA being amplified using UBC809. There was only one polymorphism with distinct bands found. The amount of polymorphism was 20%; four monomorphic bands and a single band, identified at a molecular size of 477 bp for the Giza 177, occurred in the sample treated with 10, 20, and 100 mg/L ZnO-NPs and MgONPs, respectively. In the instance of the UBC823 primer, there were a total of eight bands; all of them displayed four monomorphic bands and ranged in size from 349 to 1403 bp. There were also two distinct bands, which were found at molecular sizes of 349 bp and 928 bp for the Giza

177. Therefore, 50% of the population was polymorphic. Ten bands in all, spanning 303 to 1377 bp, were detected for the UBC807 primer (four polymorphic, six monomorphic, and 40% polymorphic). While being missing at all concentrations of ZnO NPs and MgONPs, two distinct bands with molecular sizes of 341 bp for the Sakha super 300 and 1130 bp for the Sakha 108 were found. A 42.86% polymorphism rate was present. Seven bands in all, ranging in size from 478 to 1363 bp, were obtained utilising UBC889 (five polymorphic, four monomorphic, and two unique bands found at 1349 bp for Giza 177 and 651 bp for Sakha 108). Therefore, 50% of the population was polymorphic. Ten bands in all, spanning 303 to 1377 bp, were detected for the UBC807 primer (four polymorphic, six monomorphic, and 40% polymorphic). While being missing at all concentrations of ZnO NPs and MgONPs, two distinct bands with molecular sizes of 341 bp for the Sakha super 300 and 1130 bp for the Sakha 108 were found. A 42.86% polymorphism rate was present. Seven bands in all, ranging in size from 478 to 1363 bp, were obtained utilising UBC889 (five

polymorphic, four monomorphic, and two unique bands found at 1349 bp for Giza 177 and 651 bp for Sakha 108). To ascertain the evolutionary relationships between the several species of barley, genetic diversity was examined in this case using the Inter-simple sequence repeat (ISSR) technique and DNA fingerprinting (Rashad et al., 2020; Guasmi et al., 2012; Lamine et al., 2015). High polymorphism was found between Egyptian barley collection accessions using ISSR-based genetic diversity analysis; this finding was similarly demonstrated for rice (Gorji et al., 2011) and orange (Izzatullayeva et al., 2014). ISSR markers were widely employed to distinguish between accessions and were occasionally even more effective than SSR markers. Numerous articles (Vaja et al., 2016) cite previous and more current studies that advocated the ISSR method as a useful tool for genotypic evaluation in a range of plant species.

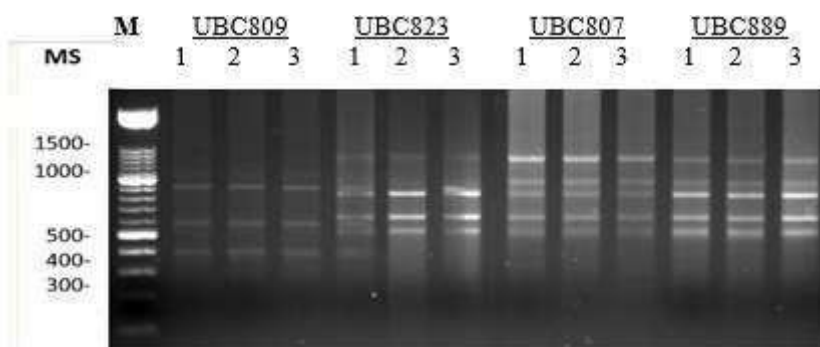


Fig. 5. Agarose gel profile of genomic DNA of Rice using ISSR-PCR markers of four primers namely (UBC809, UBC823, UBC807 and UBC889). Lane numbers represent serial number of control and different concentration (mg/L) of ZnO NPs and MgONPs. M= molecular marker ladder (1500 bp).

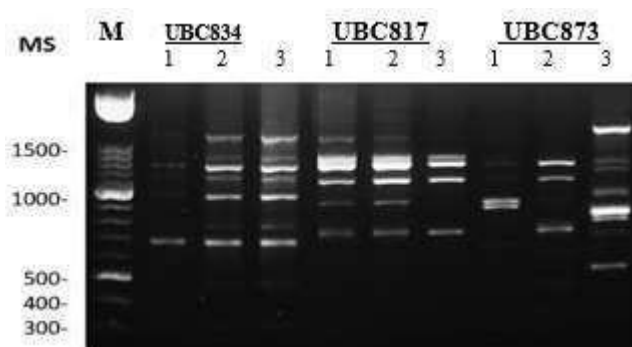


Fig.6. Agarose gel profile of genomic DNA of Rice using ISSR-PCR markers of three primers namely (UBC834, UBC817 and UBC873). Lane numbers represent serial number of control and different concentration (mg/L) of ZnO NPs and MgONPs. M= molecular marker ladder (1500 bp).

Table 2. List of ISSR primers and positive markers of three rice varieties

Primer code	MS	Giza 177	Sakha super 300	Sakha 108	Positive markers (P+*)
UBC809	477	1	0	0	1P+
UBC823	349	1	0	0	2P+
UBC807	341	0	1	1	2P+
UBC889	651	0	0	1	2P+
UBC817	1800	0	1	0	1P+
UBC873	1715	0	0	1	4P+
	793	0	0	1	
	518	0	0	1	

*P+: positive markers

RAPD markers:

The SBSC-18 primer produced six bands with a 33.33% polymorphism rate. Four monomorphic bands and

two polymorphic bands, ranging in size from 490 to 1320 bp, were discovered in this profile. For the Sakha 108, a single distinct band with a molecular size of 977 bp was found; however, it was not present at any concentration of ZnO NPs or MgONPs. The findings collected revealed that the level of polymorphism in the primers SBSF-14 and ranged from 429 to 1511 bp, while showing five monomorphic and five polymorphic bands as well as two unique bands; found at molecular sizes of 890 bp and 535 bp for the Giza 177 (Table 1&3 and Figure 7).

The two most used techniques for determining genetic differentiation across and within plant populations are RAPD and ISSR (3, 4). Using RAPD primers, more polymorphic loci (56.68%) were discovered than with ISSR primers (52.24%). The usefulness of both marker techniques in examining the genetic diversity of sunflowers was illustrated by a dendrogram made using RAPD, ISSR primers, and pooled data (Merwad et al., 2020). Studies on the genotoxic effects of NPs on plants have recently started to appear. According to Remédios et al. (2012), the term "genotoxicity" refers to the property of chemical agents that alter the genetic material within a cell and result in mutations. As a sensitive technique that may identify differences in genome profiles, randomly amplified polymorphic DNA- polymerase chain reaction (RAPD-PCR) is employed for DNA analysis in the field of genotoxicity in various plants (Kekec et al., 2010).

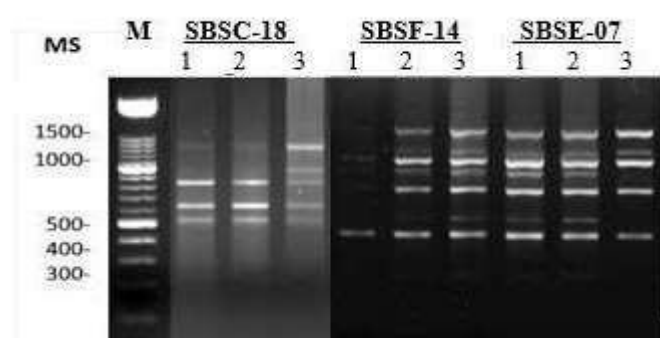


Fig.7. Agarose gel profile of genomic DNA of Rice using RAPD-PCR markers of three primers namely (SBSC-18, SBSF-14 and SBSE-07). Lane numbers represent serial number of control and different concentration (mg/L) of ZnO NPs and MgONPs. M= molecular marker ladder (1500 bp).

Table 3. List of RAPD primers and positive markers of three rice varieties

Primer code	MS	Giza 177	Sakha super 300	Sakha 108	Positive markers (P+*)
SBSC-18	977	0	0	1	1P+
SBSF-14	890	1	0	0	2P+
	535	1	0	0	
	1634	0	1	0	
	1340	0	1	0	
	1179	1	0	0	
SBSE-07	1063	0	1	0	9P+
	897	0	1	0	
	782	0	1	0	
	721	0	1	0	
	553	0	0	1	
	510	0	1	0	

*P+: positive markers

Genetic diversity and relationships

Seven ISSR and three RAPD markers from three different rice species were clustered using the UPGMA method, resulting in a dendrogram (Fig. 8). There were two clusters with high genetic similarity; Cluster A had one genotype that was subdivided using Sakha super 300. At a phylogenetic distance, Sakha 108 and Giza 177 were found to be clustered together.

The phenogram revealed two different clusters with genetic similarity scores ranging from 0.90 to 1.00. The Sakha super 300 and Giza 177 genotypes had a maximum genetic similarity coefficient of 0.95, indicating a high degree of genetic closeness. As shown in Table 4, the accessions Sakha 108 and Giza 177, both of which were towed, had the lowest closeness ratio of 0.90%.

Wheat has also been classified as following to this pattern of geographically linked grouping using molecular markers (Strelchenko et al., 1999). However, our results refute previous research on barley and *Aegilops* that claims the molecular clustering of barley does not represent its origin (Owuor et al., 2003; Mahjoub et al., 2009). Seven ISSR primers also found 37 polymorphic bands, indicating a high level of polymorphism (87.5%), and the results showed highly polymorphic profiles. According to Dakir et al. (2002), the polymorphism of Moroccan barley is 60% lower than usual.

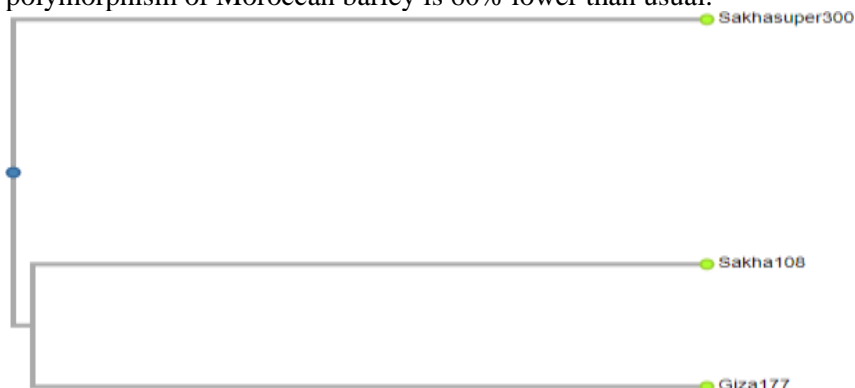


Fig. 8. Dendrogram using UPGMA cluster for 6 quantitative morphological traits of 7 *Hordeum vulgare* L.

Table 4. Similarity index among 7 accessions of *Hordeum vulgare* L. based on 6 qualitative morphological traits.

Case	Giza 177	Sakha super 300	Sakha 108
Giza177	1		
Sakha super 300	0.95	1	
Sakha 108	0.90	0.91	1

Recently, there was discussion over ZnO's ability to inhibit the growth of pathogens. Ag is probably not the best option for controlling fungal pathogens; ZnO NPs are (Dimkpa et al., 2013). For instance, ZnO NPs showed greater in vitro suppression of *Helmentosporium oryzae* and *F. graminearum* (Dimkpa et al., 2013; Elamawi et al., 2016). Biosynthesized ZnO NPs (25 g/mL) showed greater inhibition rates against harmful bacteria and fungal species in a related investigation (Jayaseelan et al., 2012). In a plating assay, ZnO NPs considerably slowed the growth of *B. cinerea* and *P. expansum* mycelia (He et al., 2011). They mentioned that these inhibitory effects interfered with cell function, led to fungal hyphal distortion in *B. cinerea*, and prevented the growth of conidia and conidiophores in *P. expansum*. The antibacterial action of ZnO NPs has been explained by a number of different mechanisms. It is thought that the production of hydrogen peroxide from the surface of ZnO NPs is an efficient method for preventing the growth of fungi. The release of Zn²⁺ ions, which can harm cell membranes and interact with intracellular components, is another potential mechanism (Sirelkhatim et al., 2015). According to Navale et al. (2015), ZnO NPs and their photo catalytic characteristics significantly contribute to their antibacterial action, inducing microbial cell membrane structural alterations, oxidative stress, and ultimately the death of the cells. Contrary to the current findings, Savi et al. (2013) state that some fungi may produce more conidia as a result of the stress brought on by ZnO NPs treatments. Fortunately, research has revealed that MgO NPs cause tomato plants to activate the salicylic acid, jasmonate, and ethylene signalling pathways (Imada et al. 2016). The good effect of MgO NPs may be attributed to their indirect enhancing effect on the action of salicylic acid, which in turn boosted the rate of cell division and accumulation of IAA in wheat seedlings (Shakirova et al., 2003).

Numerous studies have been done on how adding Zn to rice crops can boost grain yield in either normal or salinity soil (Swamy et al., 2016; Elamawi et al., 2016). This work unequivocally showed that ZnO NPs might be an effective fertiliser and antifungal agent against pathogenic fungus that can aid in preventing *M. oryzae* crop infestation. In the case of the rice cultivars Giza 177, Sakha super 300, and Sakha 108, using seven ISSR primers and three RAPD primers with 24 unique bands, the obtained results using molecular markers confirmed that the lower concentrations of ZnO-NPs and MgO nanoparticles (10 and 20 mg/L) are considered to be a good enhancement agent. These findings generally indicated that lower ZnO and MgO NP concentrations might be used as an efficient nanofertilizer for sustainable agriculture and food safety, as well as an antifungal agent for the rice fungus *Fusarium moniliforme* (Elamawi et al., 2019).

4. Conclusion

When applied at the right concentration and timing, foliar application of ZnO and MgO nanoparticles on rice cultivars (Giza 177, Sakha super 300, and Sakha 108) offers a practical and useful approach to enhance rice plant performance and productivity while mitigating leaf blast. On rice cultivars iza 177, Sakha super 300, and Sakha 108, molecular markers are regarded as useful instruments and proof of the enhancing effects of lower concentrations of ZnO and MgO nanoparticles. Additionally, it increased the grain production of the rice cultivar and had inhibitory effects on *Fusarium moniliforme*.

Conflicts of interest

The authors declare there are no conflicts of interest.

References:

1. Khush, G.S (2005). What it will take to feed 5.0 billion rice consumers in 2030. *Plant Mol. Biol.*, 59, 1–6. [CrossRef] [PubMed]
2. Khan, F.; Naaz, S.; Singh, N.; Shukla, P.K.; Tripathi, R.; Yadav, H.K.; Shirke, P.A. (2022)Molecular, physiological and agronomic assessment of genetic diversity in rice varieties in relation to drought treatment. *Curr. Plant Biol.*, 29, 100232. [CrossRef]
3. El-Mowafi, H.F.; AlKahtani, M.D.; Abdallah, R.M.; Reda, A.M.; Attia, K.A.; El-Hity, M.A.; El-Dabaawy, H.E.; Husnain, L.A.; Al-Ateeq, T.K.; EL-Esawi, M.A. (2021). Combining ability and gene action for yield characteristics in novel aromatic cytoplasmic male sterile hybrid rice under water-stress conditions. *Agriculture*, 11, 226. [CrossRef]
4. Faostat. (2022). Food and Agriculture Organization of the United Nations. Statistical Database.. Available online: <http://www.fao.org/faostat/en/#data>.
5. Fageria, N. (2007). Yield physiology of rice. *J. Plant Nutr.*, 30, 843–879. [CrossRef]
6. Rastogi, A.; Kumar, D.; Saurabh, T.; Devendra, Y.; Chauhan, K.; and Živč k, M. (2019). Application of silicon nanoparticles in agriculture. *Biotech.*, 9: 1-11.
7. Youssef, M.S. and Elamawi, R.M. (2018). Evaluation of phytotoxicity, cytotoxicity, and genotoxicity of ZnO nanoparticles in *Vicia faba*. *Environ. Sci. Pollut. Res. Int.*, 27(16): 18972-18984.
8. FAO. (2009). FAO's director-general on how to feed the world in 2050. Insights from an Expert Meeting at FAO. FAO. 1:1-35.
9. Couch, B.C. and Kohn, L.M. (2002). A multilocus gene genealogy concordant with host preference indicates segregation of a new species, *Magnaporthe oryzae*, from *M. grisea*. *Mycologia*. 94: 683-693.
- 10.Ou, S.H. (1985). *Rice Diseases*. Commonwealth Agricultural Bureaux,2nd ed., pp. 380.
- 11.Nirenberg, H. I. (1976). Untersuchungen uber die morpholoigische und biologische Differenzierung in der *Fusarium*- Sektion *Liseola*. *Mitt. Biol. Bundesanst. Land-u. Forstwirtsch. Berlin-Dahlem*, 169, 1-117.
- 12.Nalley, L.; Tsiboe, F.; Durand-Morat, A.; Shew, A. and Thoma, G. (2016). Economic and environmental impact of rice blast pathogen (*Magnaporthe oryzae*) alleviation in the United States. *PLoS One*. 11(12): e0167295.
- 13.Young, J.; Byung, K. and Geunhwa, J. (2009). Antifungal activity of silver ions and nanoparticles on phytopathogenic fungi. *Plant Dis.*, 93: 1037-1043.
- 14.Elamawi, R.M. and El-Shafey, R.A. (2013). Inhibition effects of Silver nanoparticles against rice blast disease caused by *Magnaporthe grisea*. *Egypt. J. Agric. Res.*, 91(4): 1271-1283
- 15.Elamawi, R.; Al-Harbi, R. and Hendi, A. (2018). Biosynthesis and characterization of silver nanoparticles using *Trichoderma longibrachiatum* and their effect on phytopathogenic fungi. *Egypt. J. Bio. Pest Cont.*, 28:28.
- 16.He, L.; Liu, Y.; Mustapha, A. and Lin, M. (2011). Antifungal activity of zinc oxide nanoparticles against *Botrytis cinerea* and *Penicillium expansum*. *Microbiol. Res.*, 166: 207-215.
- 17.Gunalan, S.; Sivaraj, R. and Rajendran, V. (2012). Green synthesized ZnO nanoparticles against bacterial and fungal pathogens. *Prog. Nat. Sci. Mater. Int.*, 22: 693-700.
- 18.Wani, A.H. and Shah, M.A. (2012). A unique and profound effect of MgO and ZnO nanoparticles on some plant pathogenic fungi. *J. Appl. Pharm. Sci.*, 2: 40-44.
- 19.Savi, G.D.; Bortoluzzi, A.J. and Scussel, V. M. (2013). Antifungal properties of Zinccompounds against toxigenic fungi and mycotoxin. *Int. J. Food Sci. Technol.*, 48: 1834-1840.
- 20.Elamawi, R.M.; Bassiouni, S.M.; Elkhoby, W.M. and Zayed, B.A. (2016). Effect of Zinc oxide nanoparticles on brown spot disease and rice productivity under saline soil. *J. Plant Prot. Path. Mansoura*

- Univ., 7(3): 171-181.
21. Sierra-Fernandez, A.; De La Rosa-García, S.C.; Gomez-Villalba, L.S.; GómezCornelio, S.; Rabanal, M.E. and Fort, R. (2017). Synthesis, photocatalytic, and antifungal properties of MgO, ZnO and Zn/Mg oxide nanoparticles for the protection of calcareous stone heritage. *ACS Appl. Mater. Interfaces.*, 9: 24873-24886
 22. Kulhare, P.; Tagore, G.; and Sharma, G. (2017). Effect of foliar spray and sources of Zinc on yield, Zinc content and uptake by rice grown in a vertisol of central India. *Inte J Chem. Stud.*, 5(2): 35-38.
 23. Al-Turki TA and Basahi MA. (2015). Assessment of ISSR based molecular genetic diversity of Hassawi rice in Saudi Arabia. *Saudi J Biol Sci.* 2015 Sep;22(5):591-9. doi: 10.1016/j.sjbs. 06.027. Epub 2015 Jul 8. PMID: 26288564; PMCID: PMC4537881.
 24. Fernandes, M., RB Singh, K., Sarkar, T., Singh, P., & Pratap Singh, R. (2020). Recent Applications of Magnesium Oxide (MgO) Nanoparticles in various domains. *Advanced Materials Letters*, 11(8), 1-10. doi: 10.5185/amlett.2020.081543
 25. Barnett, H. L., & Hunter, B. B. (1972). *Illustrated genera of imperfect fungi. Illustrated genera of imperfect fungi.*, (3rd ed).
 26. Nelson, P. E., Toussoun T. A., and Marasas W. F. O. (1983) *Fusarium species: an illustrated manual for identification.* The Pennsylvania State University Press, University Park.
 27. Gardes, M., & Bruns, T. D. (1993). ITS primers with enhanced specificity for basidiomycetes-application to the identification of mycorrhizae and rusts. *Molecular ecology*, 2(2), 113-118.
 28. Castillo, Jose Antonio & Conde, Giovanna & Claros Magnus, Mayra & Ortuño Castro, Noel. (2022). Diversity of cultivable microorganisms associated with Quinoa (*Chenopodium quinoa*) and their potential for plant growth-promotion. *Revista Bionatura*.
 29. White, T.J. (1990) Amplification and Direct Sequencing of Fungal Ribosomal RNA Genes for Phylogenetics. In: *PCR Protocols, a Guide to Methods and Applications*, 315-322.
 30. Williams JG, Kubelik AR, Livak KJ, Rafalski JA, Tingey SV (1990). DNA polymorphisms amplified by arbitrary primers are useful as genetic markers. *Nucleic Acids Res.* Nov 25; 18(22): 6531-5. doi: 10.1093/nar/18.22.6531. PMID: 1979162; PMCID: PMC332606.
 31. Heibal S. A.A., Rania Tawfick Ali1, Hamdy M. Abdel-Rahman*1 and Shimaa E. Rashad2. (2022). Detected molecular markers for Alfalfa (*Medicago sativa*) using ISSR and SSR under Egyptian conditions. *International Journal of Latest Technology in Engineering, Management & Applied Science (IJLTEMAS)*; XI, XI, 2278-2540
 32. Zietkiewicz, E., Rafalski, A., Labuda, D (1994). Genome fingerprinting by simple sequence repeat (SSR)-Anchored Polymerase Chain Reaction Amplification. *Genomics*. 20, 176-183.
 33. Sambrook, J., Fritsch, E. R., & Maniatis, T. (1989). *Molecular Cloning: A Laboratory Manual* (2nd ed.). Cold Spring Harbor, NY: Cold Spring Harbor Laboratory Press.
 34. Norman N, H (1975). *Spss Statistical Package for the Social Sciences*, Second Edition. New York: McGraw- Hill Book Co., *Journal of Advertising*, 5:1, 41-42, DOI: 10.1080/00913367.1976.10672624
 35. Gomez K. A. and Gomez A. A. (1984). *Statistical procedures for agricultural research.* John Wiley & sons. P. 180.
 36. Rashad S. E.*1, F. M. Abdel-Tawab 3, Eman M. Fahmy3, Saker, M. M2. (2020). Somaclonal variation from mature embryo explants of some Egyptian barley genotypes. *Egypt. J. Genet. Cytol.*; 49:103-121.
 37. Rashad S. E., El- Demerdash I. S., Abdel-Rahman H. M., EL-Enany, M. A. M, Heiba S. A. A. (2023). Screening of genetic diversity in Seventeen sunflower (*Helianthus annuus* L.) genotypes for oil content and the early flowering rate using RAPD markers
 38. Merwad M.A.1; E.A.M. Mostafa1; N.E. Ashour1; M.M.S. Saleh1; Ibthal S. El- Demerdash2 and Shimaa E. Rashad*3.(2020). Horticultural Studies And Genetic Relationship Via Dna Fingerprinting Using RAPD Markers Between Sewi Date Palm And Two Superior Seeded Females. *Plant Cell Biotechnology And Molecular Biology*; 22 (59&60): 56-66.
 39. Shata S. M. 1,* , Said W. M. 1 , Abdel-Tawab F. M. 2 , Kamal L. M. 2. (2021). Morphological and Quantitative traits of phylogenetic relationships of some barley (*Hordeum vulgare* L.) accessions in Egypt.- *Journal of Scientific Research in Science*; 38, (1): 16-35
 40. Rashad S. E., El- Demerdash I. S., Abdel-Rahman H. M., EL-Enany, M. A. M, Heiba S. A. A. (2023). Enhancement of some barley (*Hordeum vulgare* L.) resistance for nematode (*Heterodera avenae*) using DNA fingerprinting analysis. *Egyptian Pharmaceutical Journal*, *in press*.
 41. Rashad S. E. a *, Samy A. A. Heiba b, Mohamed A. Emam c, Samira A. Osman and Ibthal Salah Eldemerdash b. (2023). Effect of PEG induced drought stress on Genetic diversity using SDS-PAGE and ISSR markers for Egyptian barley varieties. *Egyptian Journal of chemistry*, *in press*.

42. Heiba S. A. A., Ibtal Salah Eldemerdash and Shima E. Rashad, (2023). Evaluation of biological control of sorghum strains using (*Bacillus thuringiensis*) and (*Pseudomonas aeruginosa*) under drought stress. *Egyptian Pharmaceutical Journal*, *in press*.
43. Petosa, A.R.; Rajput, F.; Selvam, O.; Öhl, C. and Tufenkji, N. 2017. Assessing the transport potential of polymeric nanocapsules developed for crop protection. *Water Res.*, 111: 10-17.
44. Guasmi, F.; Elfalleh, W.; Hannachi, H.; Feres, K.; Touil, L.; Marzougui, N.; Triki, T.; Ferchichi, A. (2012). The use of ISSR and RAPD markers for genetic diversity among south tunisian barley. *ISRN Agron.*, 1–10. [Google Scholar] [CrossRef][Green Version]
45. Lamine M, A Mliki, (2015). Elucidating genetic diversity among sour orange rootstocks: a comparative study of the efficiency of RAPD and SSR markers, *applied biochemistry and biotechnology*; 175: 2996-3013
46. Gorji AM, P Poczai, Z Polgar, J Taller (2011). Efficiency of arbitrarily amplified dominant markers (SCoT, ISSR and RAPD) for diagnostic fingerprinting in tetraploid potato, *American journal of potato research*; 88: 226-237
47. Izzatullayeva V, Z. Akparov, S. Babayeva, J. Ojaghi, M. Abbasov (2014). Efficiency of using RAPD and ISSR markers in evaluation of genetic diversity in sugar beet, *Turkish Journal of Biology*; 38: 429-438
48. Vaja KN, HP Gajera, ZA Katakpara, SV Patel, BA Golakiya (2016). Biochemical indices and RAPD markers for salt tolerance in wheat genotypes, *Indian Journal of Plant Physiology*; 21: 143-150
49. Elamawi, R., Youssef, M., & EL-Refae, Y. (2019). Estimate of the Antifungal Activity and Phytotoxicity of ZnO Nanoparticles on *Magnaporthe oryzae* and Rice Cultivar Sakha 101 using Morphological, Biochemical and Molecular Markers. *Egyptian Journal of Phytopathology*, 47(1), 1-29. doi: 10.21608/ejp.2019.119996
50. Remédios, C.; Rosário, F. and Bastos, V. 2012. Environmental nanoparticles interactions with plants: morphological, physiological, and genotoxic aspects. *J. Bot.*, 2012: 1-8.
51. Kekec, G., Sakcali, M. S. and Uzonur, I. 2010. Assessment of genotoxic effects of boron on wheat (*Triticum aestivum* L.) and Bean (*Phaseolus vulgaris* L.) by using RAPD analysis. *Bull. Environ. Contam. Toxicol.*, 84: 759-764.
52. Strelchenko P, O Kovalyova, K Okuno. (1999). "Genetic differentiation and geographical distribution of barley germplasm based on RAPD markers." *Genetic resources and crop evolution*; 46: 193-205.
53. Owuor ED, A Beharav, T Fahima, VM Kirzhner, AB Korol, E Nevo, (2003). Microscale ecological stress causes RAPD molecular selection in wild barley, Neve Yaar microsite, Israel, *Genetic Resources and Crop Evolution*; 50: 213-224
54. Mahjoub A, MS El Gharbi, K Mguis, M El Gazzah, NB Brahim, (2009). Evaluation of genetic diversity in *Aegilops geniculata* Roth accessions using morphological and RAPD markers, *Pakistan journal of biological sciences: PJBS*; 12: 994-1003
55. Dakir EH, ML Ruiz, P García, MP de la Vega, (2002). Genetic variability evaluation in a Moroccan collection of barley, *Hordeum vulgare* L., by means of storage proteins and RAPDs, *Genetic Resources and Crop Evolution*; 49: 619-631